Quantitative Clinical Pharmacology Supports the Bridging From i.v. Dosing and Approval of s.c. Rituximab in B-Cell Hematological Malignancies

Candice Jamois[1,*], Ekaterina Gibiansky[2], Leonid Gibiansky[2], Clarisse Chavanne[1], Peter N. Morcos[1], Christine McIntyre[3], Martin Barrett[3], Linda Lundberg[4], Artem Zharkov[5], Axel Boehnke[4] and Nicolas Frey[1]

A fixed-dose subcutaneous (s.c.) formulation of the anti-CD20 antibody, rituximab, has been developed to address safety, infusion time, and patient comfort concerns relating to intravenous (i.v.) dosing, and has been approved based upon a pharmacokinetic (PK)–clinical bridging strategy, which demonstrated noninferiority of s.c. vs. i.v. dosing in malignancies, including follicular lymphoma (FL) and chronic lymphocytic leukemia (CLL). A clinical development plan was undertaken to identify rituximab s.c. doses achieving noninferior exposure to rituximab i.v., and to confirm PK–clinical bridging, with the same efficacy and similar safety. This drew upon data from 1,579 patients with FL, CLL, or diffuse large B-cell lymphoma in 5 clinical studies, and showed minimum steady-state serum concentration (C_{trough}) as the most appropriate exposure bridging measure. Population PK models were developed, simulations were run using covariates and PK parameters from clinical studies, and exposure–efficacy and –safety analyses performed. Population PKs showed a two-compartment model with time-dependent and -independent clearances. Clearance and volume were predominantly influenced by body surface area; disposition and elimination were similar for the s.c. and i.v. formulations. After s.c. administration, patients with FL and CLL achieved noninferior exposures to i.v. dosing. Overall, rituximab exposure and route of administration did not influence clinical responses in patients with FL or CLL, and there was no association between exposure and safety events. C_{trough} was shown to be an effective pharmacologic–clinical bridging parameter for rituximab in patients with FL or CLL. Clinically effective exposures are achieved with either s.c. or i.v. dosing.

Study Highlights

WHAT IS THE CURRENT KNOWLEDGE OF THE TOPIC?

☑ The anti-CD20 antibody rituximab (R) is standard-of-care in a number of B-cell malignancies, and has been available since 1997 for intravenous (i.v.) infusion. A subcutaneous (s.c.) formulation, designed to address concerns over clinic and patient time/convenience, and aspects of safety related to i.v. infusion, has been approved.

WHAT QUESTION DID THIS STUDY ADDRESS?

☑ R-s.c. is given by fixed-dose administration. Population pharmacokinetic (PopPK) models with exposure measures to bridge the i.v. and s.c. formulations were developed to assist optimization of dosing.

WHAT DOES THIS STUDY ADD TO OUR KNOWLEDGE?

☑ This analysis shows minimum serum drug concentration across the approved doses and dosing intervals (C_{trough}) to be an effective primary end point for bridging R-s.c. and R-i.v. R-s.c. confers noninferior exposure and anti-lymphoma activity vs. R-i.v., with similar clinical benefit and safety.

HOW MIGHT THIS CHANGE CLINICAL PHARMACOLOGY OR TRANSLATIONAL SCIENCE?

☑ Our results confirm the utility of bridging studies based on PopPK models using integration of PKs, efficacy, and safety data, and are a good example of model-informed drug development.

[1]Clinical Pharmacology, Pharmaceutical Sciences, Pharma Research and Early Development, Roche Innovation Center Basel, Basel, Switzerland; [2]QuantPharm LLC, North Potomac, Maryland, USA; [3]Pharma Research and Early Development, Roche Innovation Center Welwyn, Welwyn Garden City, UK; [4]Pharma Development Clinical Oncology, F. Hoffmann-La Roche Ltd, Basel, Switzerland; [5]Pharma Development Medical Affairs, F. Hoffmann-La Roche Ltd, Basel, Switzerland. *Correspondence: Candice Jamois (candice.jamois@roche.com)

Received February 25, 2021; accepted April 25, 2021. doi:10.1002/cpt.2308

Rituximab (MabThera®/Rituxan®) is a chimeric murine/human monoclonal antibody (mAb) that binds to the transmembrane CD20 antigen on the surface of normal and malignant B cells, exerting its anti-B-cell activity via antibody-dependent cellular cytotoxicity, complement-dependent cytotoxicity, induction of apoptosis, and phagocytosis of opsonized targets such as macrophages.[1,2] B-cell progenitors in bone marrow lack CD20, allowing healthy B cells to regenerate after treatment and return to normal levels within several months.[3] Initially formulated for intravenous infusion, rituximab (R-i.v.) was the first anticancer mAb approved in the United States (1997) and Europe (1998). Rituximab has transformed outcomes in B-cell malignancies, and is standard-of-care for non-Hodgkin lymphoma (NHL; follicular lymphoma (FL) and diffuse large B-cell lymphoma), and chronic lymphocytic leukemia (CLL).[4–7]

To address treatment burden associated with lengthy infusions, and potential for severe administration reactions,[8–10] a subcutaneous formulation (R-s.c.; MabThera® s.c./Rituxan Hycela®) that formulates standard rituximab with recombinant human hyaluronidase[11–13] was developed, and is approved in the United States[14] and the European Union.[10] US approval followed an Oncology Drug Advisory Committee (ODAC) review of the novel clinical development program, which focused primarily on a pharmacokinetic (PK)-based clinical bridging approach to demonstrate PK noninferiority of s.c. vs. i.v. dosing in NHL and CLL.[1,15] Notably, the ODAC ultimately established precedence for other biologics to use a similar PK–bridging development program to introduce s.c. routes of administration (e.g., trastuzumab).[16,17] Herein, we describe the integration of PK, safety, and efficacy data in a model-informed manner through quantitative clinical pharmacology (qCP) techniques (population PK (PopPK) and exposure–response (ER) analyses),[18] and provide the scientific evidence that supported the regulatory acceptance of the R-s.c. formulation in FL and CLL.

METHODS

R-s.c. clinical development plan

The clinical development plan aimed to (i) identify R-s.c. doses achieving noninferior exposure to R-i.v., (ii) confirm PK–clinical bridging, (iii) establish comparability of safety and effectiveness, and (iv) evaluate patient satisfaction and preference for administration route. The plan drew upon data from 1,579 patients with FL, diffuse large B-cell lymphoma, or CLL in 5 clinical trials,[19–25] described in the **Supplementary Methods**.

Three of the trials, SparkThera,[21] SABRINA,[19,20] and SAWYER,[22,24] were designed specifically as PK noninferiority studies to ensure noninferior exposure when treating patients with R-s.c. compared with R-i.v., and supported the PK–clinical bridging analyses. SABRINA, SAWYER (stage 2), PrefMab, and MabEase also supported evaluation of R-s.c. efficacy and safety.[1,19,20,23–26] SparkThera and SAWYER were two-stage studies of R-s.c. vs. R-i.v. in FL and CLL, respectively; stage 1 was dose-finding, whereas the primary objective of stage 2 was to demonstrate noninferiority of R-s.c. vs. R-i.v. (dose-confirmation).[21,22,24] SABRINA was a two-stage study of R-s.c.- vs. R-i.v.-based chemoimmunotherapy induction (given every 3 weeks (Q3W)) followed by maintenance (every 2 months (Q2M)) with R-s.c. or R-i.v. in patients with FL; the primary end points were minimum steady-state serum rituximab concentration (C_{trough}) at cycle (C)7 (stage 1)[19] and efficacy (overall response rate at end of induction (EOI); stage 2).[20]

The qCP analyses leveraged R-i.v. single-dose data in patients with FL undergoing maintenance treatment (from the approved dose of 375 mg/m^2 to 800 mg/m^2) to inform the 1,400 mg R-s.c. dosing in the "pivotal" dose-confirmation study parts (SparkThera stage 2 and SABRINA stage 1; data not shown). Thus, SparkThera stage 2 and SABRINA stage 1 supported the Q3W and Q2M dosing schedules for induction and maintenance treatment, respectively, in FL, and were ultimately used to support the rituximab label in NHL.[1] Similarly, SAWYER stage 2 confirmed 1,600 mg 4-weekly (Q4W) s.c. dosing in CLL.[24]

PK analysis

Because of rituximab's mode of action and its known target-mediated drug disposition (TMDD),[27] sustained saturation of B-cell CD20 receptors obtained with the R-i.v. regimen is due to sufficient rituximab serum concentration levels maintained over a dosing interval.[28] C_{trough} correlates with efficacy,[29–31] and similar C_{trough} levels across formulations would be expected to achieve comparable efficacy and safety. Therefore, C_{trough} was considered the appropriate PK exposure measure to bridge from i.v. to s.c. administration. Furthermore, rituximab is known to have a wide therapeutic window, making it a suitable candidate for fixed-dose s.c. administration (studies of i.v. administration evaluated concentrations up to 2,200 mg/m^2).[32,33]

A PopPK model in CLL was previously established[26] using data from two trials, REACH (phase III, relapsed/refractory setting),[34] and SAWYER (phase Ib, previously untreated).[24] Following i.v. administration, rituximab PKs were described by a two-compartment model with clearance consisting of two components: a time-dependent component (CL_T) corresponding to the decrease in capacity of a target-mediated clearance pathway, and a second component, independent of time (CL_{inf}) and related to the endogenous catabolic processes of IgG, which is impacted by the neonatal Fc receptor:

$$CL = CL_T \times \exp(-k_{des} \times t) + CL_{inf}$$

Where k_{des} is the rate constant of decay of CL_T with time (t).

In FL, a PopPK analysis based on data from the phase Ib SparkThera trial[21] was re-evaluated with data from the phase III SABRINA registration trial[19,20] and is presented here.

Interactions between covariates (e.g., body surface area (BSA), age, baseline B-cell count, tumor size, white blood cell count , and serum albumin concentration, presence of antidrug antibodies) and PK parameters were identified by scientific interest, mechanistic plausibility, and exploratory graphics, and were included in covariate model development.

Interpretation and refinement of the models were based on point estimates, confidence intervals (CIs), and diagnostic plots of the covariate effects. Precisely estimated but clinically insignificant effects and those not supported by data (e.g., effects close to null value, with high relative standard error or CIs including the null value) were excluded. Analyses in CLL and FL were conducted using NONMEM software (ICON Development Solutions).[35] Details of dosing, patient numbers, and PK sampling are shown in **Table S1**.

Simulations

To compare rituximab exposure across the formulations, simulations were conducted with the two PopPK models, using covariate factors and individual PK parameters from patients who received ≥ 1 rituximab s.c. dose in SABRINA or SAWYER. Rituximab dosing intervals and treatment durations differed for SAWYER (CLL; Q4W for 6 cycles) and SABRINA (FL; Q3W for 8 cycles followed by Q2M maintenance for ≤ 2 years; **Table S1**).

Rituximab exposure measures at C6 (predose; CLL) and end of C7 (FL) were C_{trough}, area under the curve of drug concentration vs. time for a dosing interval (AUCτ), maximum serum concentration (C_{max}),

individual ratios of s.c. to i.v. exposures, and proportion of patients with i.v.:s.c. ratio < 1. The measures were predicted using both models, summarized for all individuals, and compared between i.v. and s.c. formulations. Times needed to saturate the time-varying elimination pathway of rituximab were also compared.[26] To assess rituximab ER relationships (safety and efficacy), C_{trough} at EOI (FL) or at the end of treatment (CLL; C_{tr}LD) and average concentrations over the induction period (C_{mean}LD) were also computed.

Exposure–efficacy analysis

Exposure–efficacy analyses in FL were conducted using data from SABRINA and SAWYER stage 2. The analyses utilized exposure measures derived from the PopPK models at the timepoint of the primary PK analysis (C_{trough} noninferiority; i.e., rituximab C_{trough} at the end of C7 of induction for FL and at C6 (predose) for CLL).

In FL, relationships among exposure, patient characteristics, or disease-specific covariates, and progression-free survival (PFS) were explored using semiparametric Cox proportional hazard (CPH) models[26] in patients who received ≥ 7 rituximab doses. The relationship between rituximab exposure (continuous variables of C_{trough} at the end of C7 (primary measure per protocol, utilizing rituximab concentration 21 days after the C7 dose), log (C_{trough} at the end of C7), AUCτ at the end of C7 (AUC7, exploratory secondary measure, AUCτ from time of C7 dose until 21 days postdose), log (AUC7), and tertiles of C_{trough} at the end of C7) and PFS was first characterized using a base CPH model (i.e., without covariates). For a small number of patients, C_{trough} was extremely low (< 5th percentile of the C_{trough} distribution at C7; **Figure S1**). After graphical exploration, it was noted that PFS for those patients was also low compared with the rest of the population; therefore, the corresponding C7 C_{trough} values were considered further. Subsequent univariate screening identified covariates that were incorporated in the full covariate model. The performance of the exposure–PFS model was evaluated using diagnostic plots and visual predictive check simulations. The list of investigated covariates and the CPH model development are described in the **Supplementary Methods**.

Details of a similar analysis conducted in patients with CLL are reported elsewhere.[26]

Integrated exposure–safety analysis

PK profiles of R-s.c.- and R-i.v.-treated patients who received ≥ 1 dose of rituximab with or without safety events were compared graphically. Selected safety data from the induction phase from patients with FL (SABRINA stages 1 and 2) and CLL (SAWYER stage 2) were combined in an integrated exposure–safety analysis based on logistic regression with bootstrapping (**Supplementary Methods**). Data from the nonrandomized SAWYER part 1 were excluded.

This analysis was conducted for serious adverse events (SAEs), grade ≥ 3 adverse events (AEs), and selected AEs of interest, including administration-related reactions (ARRs (any AE occurring within 24 hours of treatment administration considered by the investigator as causally related to treatment)), neutropenia (including febrile neutropenia) and serious infections and infestations defined as AEs in the Medical Dictionary for Regulatory Activities System Organ Class "Infections and Infestations." For each safety end point, C_{tr}LD and C_{mean}LD were investigated as measures of exposure for i.v. and s.c. concentrations for each study separately and for the two studies combined (**Supplementary Methods**).

RESULTS

PopPK analysis and simulations

The FL PopPK analysis was based on data from 8,163 quantifiable serum concentrations from 399 patients (SABRINA stages 1 and 2) with ≥ 1 quantifiable rituximab serum concentration. Of these patients, 196 received ≥ 1 R-s.c. dose and 203 received only R-i.v. doses (all patients received their first dose as R-i.v.). The CLL PopPK model is reported elsewhere (based on 4,739 concentrations from 255 patients).[26]

A two-compartment PopPK model with combined CL_T and CL_{inf} clearances, additional nonlinear elimination, and first-order s.c. absorption, was used to describe rituximab serum concentrations for both formulations in patients with FL. The CL_T component of the clearance declined exponentially with time (k_{des}); this elimination pathway is thought to represent binding to the CD20 target present on peripheral B cells. An additional nonlinear elimination component throughout a new compartment (possibly representing elimination through a nonrenewable target) was added to the model and described by Michaelis–Menten elimination with V_{max}, the rate of target-mediated elimination, and k_{Vmax}, the rate of depletion of this nonrenewable target (**Table 1** and **Figure 1a**). Model-based conditional simulations were used to illustrate the contribution of each component (CL_{inf}, CL_T, and V_{max}) to rituximab elimination, and consequently to its exposure (following 7 i.v. doses, 75%, 8%, and 17% of rituximab was eliminated by CL_{inf}, CL_T, and V_{max}, respectively, whereas following 7 s.c. doses, 78%, 7%, and 15% was eliminated, respectively; **Figure 1b,c**).

The model included random effects on clearance parameters (CL_{inf}, CL_T, and k_{des}), central volume of distribution (V_c), absorption rate, and residual error. Distributions of random effects were close to normal (**Figure S2**), and shrinkage of the random effects was low, < 25% for all parameters except random effect on the absorption rate constant (k_a), where it was moderate (34.4%; **Figure S3** and **Table 1**). No correlations unaccounted for by the model were observed (**Figure S4**). The NONMEM code for the final model is shown in **Table S2**.

BSA was the main covariate impacting clearance and volume parameters. CL_T increased in patients with higher baseline B-cell count and tumor size. (V_c) and k_a following s.c. dosing were dependent on age. The covariates' effects in the final model are summarized in **Table S3** and **Figure S5**. Disposition and elimination parameters of rituximab were similar for R-s.c. and R-i.v. in both FL and CLL populations. Parameter estimates from the final PopPK model in FL are shown in **Table 1**.

Despite the BSA effect on clearance and volume parameters, the simulations show that s.c. flat-dosing could be used. For both FL and CLL, flat s.c. dosing leads to larger differences in exposure between patients with low and high BSA than BSA-adjusted i.v. dosing; however, it maintains rituximab exposure for all BSA groups at levels reached by i.v. dosing, thus achieving noninferior target saturation. PK measures following i.v. and s.c. regimens for patients with FL from SABRINA are compared in **Table 2** (overall and by BSA tertiles). Fixed-dose R-s.c. 1,400 mg ensured adequate exposure to rituximab in all patients across the entire BSA range.

The covariates and individual random effects of the patients with FL who contributed to the PopPK analysis were used to compute the individual rate of decline of the CL_T (k_{des} parameter) values. This analysis showed a similar rate of decline for both R-i.v. ($N = 203$) and R-s.c. regimens ($N = 196$), with geometric means of 0.074 (coefficient of variance (CV), 0.870) vs. 0.063 (CV, 0.908) per day, respectively (comparable time needed to saturate the CL_T pathway, i.e., ≈ 5 × 9.4 and 11 days for the R-i.v. and R-s.c. regimens, respectively). The PK simulations also showed that the

Table 1 Parameter estimates from the final rituximab PopPK model in patients with FL

Parameter		Estimate	% RSE	95% CI
k_{des} (1/day)	θ_1	0.0745	8.57	0.062, 0.087
CL_T (mL/day)	θ_2	398	11.1	311, 485
CL_{inf} (mL/day)	θ_3	200	1.78	193, 207
V_C (mL)	θ_4	4540	2.20	4350, 4740
V_P (mL)	θ_5	4270	1.61	4140, 4400
Q (mL/day)	θ_6	573	3.59	533, 613
k_a (1/day)	θ_7	0.344	7.17	0.295, 0.392
F_{SC}	θ_8	0.646	0.992	0.634, 0.659
K_{Vmax} (10^{-5} ng/mL/day) 1/(ng/mL)	θ_9	9.73	3.94	8.98, 10.5
V_{max} (1/day)	θ_{10}	0.0187	4.5	0.0171, 0.0204
$V_{C,AGE}$	θ_{11}	0.211	23.9	0.112, 0.309
$k_{a,AGE}$	θ_{12}	–2.40	22.1	–3.45, –1.36
$CL_{BSA} = CL_{T,BSA} = Q_{BSA}$	θ_{13}	1.54	8.25	1.29, 1.79
$V_{C,BSA} = V_{P,BSA}$	θ_{14}	1.25	4.69	1.14, 1.37
σ_L	θ_{15}	0.602	6.94	0.52, 0.684
σ_H	θ_{16}	0.113	3.00	0.106, 0.119
σ_{50}	θ_{17}	4.41	12.6	3.32, 5.49
$k_{des, BSIZ}$	θ_{18}	–0.424	17.4	–0.568, –0.279
$CL_{T, BSIZ}$	θ_{19}	0.355	20.2	0.215, 0.496
$CL_{T, B\text{-}cell}$	θ_{20}	0.683	12.1	0.522, 0.845

Parameter		Estimate	% RSE	95% CI	Variability	Shrinkage (%)
ω^2_{kdes}	Ω (1,1)	1.07	14.5	0.765, 1.37	CV = 103%	23.1%
ω^2_{CLT}	Ω (2,2)	2.01	11.8	1.55, 2.48	CV = 142%	15.4%
ω^2_{CLinf}	Ω (3,3)	0.0776	8.07	0.0653, 0.0898	CV = 27.9%	3.8%
ω^2_{Vc}	Ω (4,4)	0.0662	12.9	0.0495, 0.0829	CV = 25.7%	20.4%
ω^2_{ka}	Ω (5,5)	0.288	17.7	0.188, 0.388	CV = 53.7%	34.4%
ω^2_{σ}	Ω (6,6)	0.136	8.32	0.114, 0.158	CV = 36.9%	2.5%
σ^2	Σ (1,1)	1	fixed			1.4%

Θ, NONMEM fixed effect parameter; Σ, residual covariance matrix; σ^2, residual variance; σ_{50}, concentrations when the SD of the exponential residual error is equal to $(\sigma_L + \sigma_H)/2$; σ_H, SDs of the exponential residual error at high concentrations; σ_L, SDs of the exponential residual error at low concentrations; Ω, interindividual covariance matrix; ω^2, interindividual variance (subscripts show the covariates of interest); BSA, body surface area; BSIZ, tumor size at baseline; CI, confidence interval; CL, clearance; CL_{BSA}, effect of BSA on clearance; CL_{inf}, nonspecific time-independent clearance; CL_T, specific time-dependent clearance; $CL_{T,BSA}$, effect of BSA on CL_T; $CL_{T,B\text{-}cell}$, effect of B cell on CL_T; $CL_{T,BSIZ}$, effect of BSIZ on CL_T; CV, coefficient of variation (100 × SD); FL, follicular lymphoma; F_{SC}, absolute subcutaneous bioavailability; k_a, subcutaneous absorption rate constant; $K_{a,AGE}$, effect of age on k_a; k_{des}, decay coefficient of time-dependent clearance; $k_{des, BSIZ}$, effect of BSIZ on k_{des}; K_{Vmax}, rate of depletion of a hypothesized nonrenewable target; PopPK, population pharmacokinetics; Q, intercompartmental clearance; Q_{BSA}, effect of BSA on Q; RSE, relative standard error (100 × standard error/parameter estimate); V_C, central volume; $V_{C,AGE}$, effect of age on V_c; $V_{C,BSA}$, effect of BSA on V_C; V_{max}, rate of target-mediated elimination; V_P, peripheral volume; $V_{P,BSA}$, effect of BSA on V_P.

proportion of rituximab eliminated through the additional nonlinear elimination component (characterized by V_{max}) was comparable between the R-i.v. and R-s.c. regimens at EOI (i.e., 17% and 15%, respectively).

To confirm the noninferiority results in FL, individual baseline covariates (BSA, B-cell count, and age) and PK parameters from 196 patients in SABRINA who received ≥ 1 R-s.c. dose were used to predict rituximab exposure after Q3W dosing. **Table 3** summarizes C_{trough}, AUCτ, and C_{max} values at induction C7 (before the last dose at C8) for the R-i.v. and R-s.c. regimens, individual s.c.:i.v. exposure ratios, and proportions of patients with s.c.:i.v. ratios < 1 and < 0.8. All patients with FL had s.c.:i.v. ratios > 1 for both pre- and postdosing at C7 for C_{trough}. A noninferiority approach based on a standard bioequivalence threshold of 0.8 demonstrated that all patients are expected to exceed the noninferiority threshold at C7 for C_{trough} (pre- and postdosing). For AUCτ, all patients are expected to have an s.c.:i.v. ratio > 0.8, and 99.5% of patients a ratio > 1.

In patients with CLL, the covariates BSA, body mass index, sex, white blood cell count, and tumor size,[26] and the individual parameters from 140 patients from SAWYER were used to predict and demonstrate that the ratios for geometric mean C_{trough} for s.c. relative to i.v. dosing exceeded 1. Similar findings were seen with AUCτ (**Table 3**). Using the threshold of 0.8, the results demonstrated that ~ 96% and 95% of patients are expected

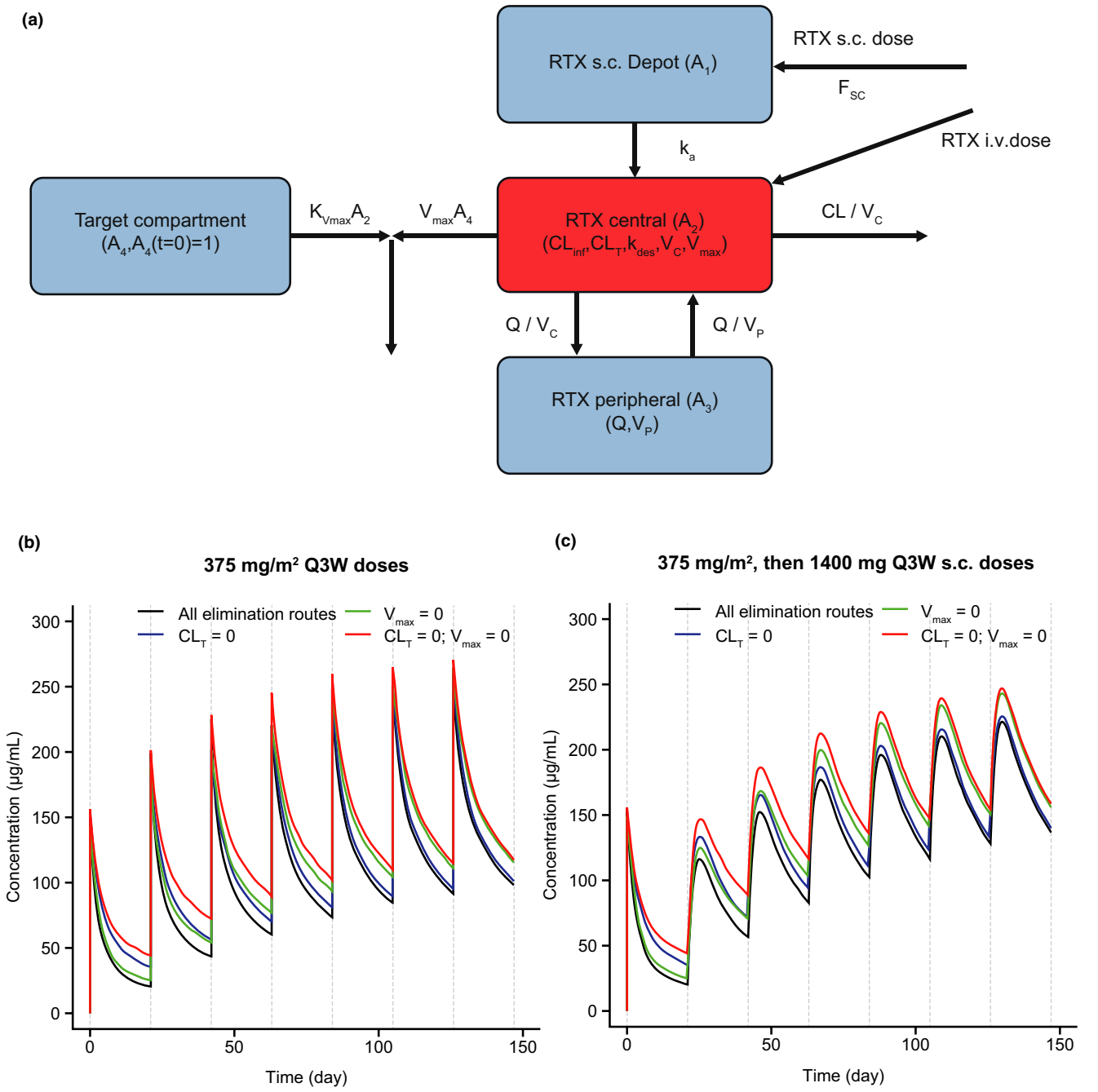

Figure 1 Scheme of the rituximab PopPK model (**a**)[a] and characterization of the contribution of each PK model component to the elimination of rituximab following i.v. (**b**)[b] and s.c. (**c**)[b] dosing in patients with FL using model-based conditional simulations. [a]Arrows pointing to the compartment indicate drug input (doses). Arrows pointing from the compartment indicate drug output (clearance). Ordinary differential equation is provided in the **Supplementary Methods**. [b]Concentration–time courses were simulated following i.v. (375 mg/m^2 C1–6) or s.c. dosing (375 mg/m^2 i.v. in C1, followed by 1,400 mg s.c. in C2–6). CL, clearance ($CL = CL_T \times \exp(-k_{des} \times t) + CL_{inf}$); CL_{inf}, time-independent clearance; CL_T, time-dependent clearance; FL, follicular lymphoma; F_{SC}, subcutaneous bioavailability; i.v., intravenous; K_a, subcutaneous absorption rate constant; k_{des}, rate constant of decay of CL_T with time; PopPK, population pharmacokinetics; Q, inter-compartmental clearance; RTX, rituximab; s.c., subcutaneous; t, time; V_C, central volume; V_P, peripheral volume; V_{max}, K_{Vmax}, target-mediated elimination from the drug and the target compartments.

to exceed the noninferiority threshold at C6 for C_{trough} for pre- and postdosing, respectively. This confirmed that nearly all patients with CLL receiving 1,600 mg R-s.c. in C2–6 would achieve C_{trough} exposures noninferior to those achieved with R-i.v.

Exposure–efficacy analysis

Patients with FL (SABRINA stage 2). The multivariate Cox regression analysis performed in 371 patients from SABRINA who received ≥ 7 rituximab doses identified that patients with

Table 2 Predicted rituximab exposure measures following i.v. and s.c. induction dosing in patients with FL from the SABRINA trial[20]

	At C7 and C8 of induction			
	C7		C8	
	i.v.	s.c	i.v.	s.c.
No. patients	203	196	203	196
C_{trough} (μg/mL)	92 (1.1–225.1)	135.2 (9.1–311)	97.8 (1.4–239.5)	145.4 (10.7–344.5)
AUCτ (μg/mL*day)	2,827 (288–5,904)	3,784 (473–7,692)	2,980 (322–6,241)	4,002 (641–8,472)

	By BSA category, at C7 and C8 of induction					
BSA category (m^2)	i.v.			s.c.		
	< 1.73	1.73–1.92	> 1.92	< 1.73	1.73–1.92	> 1.92
No. patients	52	77	74	76	54	66
C_{trough}, pre-C8 dose (i.e., C7) (μg/mL)	95.9 (3.44–196)	95.9 (6.31–217)	84.2 (1.1–225)	182 (9.07–311)	122 (34.8–303)	118 (9.86–233)
C_{trough}, post-C8 dose (μg/mL)	103 (4.85–212)	101 (8.29–230)	87.5 (1.44–239)	192 (10.7–345)	133 (45.5–336)	126 (15.9–254)
AUCτ (μg/mL*day)	3,110 (546–5,370)	3,070 (698–6,080)	2,770 (322–6,240)	5,060 (685–8,470)	3,700 (1,770–7,480)	3,440 (641–6,330)

Results are median (range). The covariate factors and individual PK parameters from patients with FL from the R-i.v. and R-s.c. arms of SABRINA were used to compute rituximab exposure metrics following the i.v. (375 mg/m^2) and s.c. (375 mg/m^2 i.v. in cycle 1, followed by 1,400 mg s.c. in cycles 2–8) dosing regimens. AUCτ, area under the curve of serum drug concentration vs. time for one dosing interval; BSA, body surface area; C, cycle; C_{trough}, trough serum rituximab concentration; FL, follicular lymphoma; i.v., intravenous; PK, pharmacokinetic; s.c., subcutaneous.

Table 3 Model-predicted PK parameters and proportion of patients with FL or CLL with lower s.c. vs. i.v. exposures at C7 (SABRINA) and C6 (SAWYER)

	i.v.	s.c.	Ratio s.c./i.v.	% of patients with s.c./i.v. ratio < 1 (90% CI)	% of patients with s.c./i.v. ratio < 0.8 (90% CI)
C7 of induction (patients with FL from SABRINA)					
Predose C_{trough} (μg/mL)	74.9 (0.629)	117 (0.575)	1.56 (0.183)	0 (0–1.8)	0 (0–1.8)
Postdose C_{trough}[a] (μg/mL)	84 (0.559)	131 (0.527)	1.55 (0.173)	0 (0–1.8)	0 (0–1.8)
AUCτ (μg/mL*day)	2,690 (0.358)	3,680 (0.399)	1.37 (0.135)	0.5 (0.0–2.7)	0 (0–1.8)
C_{max} (μg/mL)	220 (0.224)	218 (0.333)	0.991 (0.179)	52.6 (46.4–58.6)	8.2 (4.9–13.1)
C6 (patients with CLL from SAWYER)					
Predose C_{trough} (μg/mL)	69.3 (0.794)	80.6 (0.753)	1.16 (0.235)	25.7 (19.8–32.6)	4.29 (1.99–8.52)
Postdose C_{trough}[b] (μg/mL)	80.7 (0.678)	93.0 (0.652)	1.15 (0.235)	27.1 (21.1–34.1)	5 (2.48–9.42)
AUCτ (μg/mL*day)	3,790 (0.409)	4,020 (0.451)	1.06 (0.245)	40.7 (33.8–48)	12.1 (8.01–17.8)
C_{max} (μg/mL)	253 (0.226)	202 (0.380)	0.796 (0.285)	75.7 (68.9–81.5)	49.3 (42.1–56.5)

Results are presented as geometric mean (CV and/or percentage (90% CI)). The CV is computed as standard deviation of the log-transformed data.
AUCτ, area under the curve of serum drug concentration vs. time for one dosing interval; C, cycle; CI, confidence interval; CLL, chronic lymphocytic leukemia; C_{max}, peak serum rituximab concentration; C_{trough}, trough serum rituximab concentration; CV, coefficient of variance; FL, follicular lymphoma; i.v., intravenous; PK, pharmacokinetic; s.c., subcutaneous.
[a]C_{trough} concentration at the end of cycle 7 (i.e., predose of cycle 8).
[b]C_{trough} concentration at the end of cycle 6 (i.e., predose of cycle 7).

a C_{trough} at the end of C7 < 34 μg/mL had a risk of progression ~ 12-fold greater (hazard ratio (HR) = 11.9) than patients with higher exposure (**Figure 2**). Only eight patients (2.2%) had such a low rituximab C_{trough}, seven of whom were from the i.v. arm. Individual PK and B-cell profiles for those patients are shown in **Table S4**. Two patients from the R-i.v. arm with a low rituximab C_{trough} had antidrug antibodies against rituximab, both of whom had a higher initial clearance that declined slowly. Of all considered

baseline covariates, only tumor size had a statistically significant effect on PFS; patients with higher tumor size had an increased risk of progression compared with other patients. Relative to the median tumor size (log[BSIZ] = 8.41), the risk of progression decreased by 35% (HR = 0.646) for the 5th percentile of tumor size (log[BSIZ] = 6.75) and increased by 52% (HR = 1.52) for the 95th percentile of tumor size (log[BSIZ] = 10; **Figure 2**).

Patients with CLL (SAWYER stage 2). Similar to FL, a Cox regression analysis performed in 145 patients with CLL from SAWYER who received 6 doses of rituximab showed that C_{trough} values at C6 (pre-dose) < 32 μg/mL (observed in 8/145 patients (5.5%), six of whom received R-i.v.) and high tumor size were associated with poorer PFS.[26]

Integrated exposure–safety analysis

Rituximab concentrations were similar among subjects with or without AEs; no association between higher exposure and specific AEs could be identified in the time course analysis. In particular, in 398 patients with FL from SABRINA, exposure–safety analyses following i.v. and s.c. dosing indicated no correlation between rituximab exposure and neutrophil counts, occurrence and grades of AEs, SAEs, serious infections, grade ≥ 3 AEs, neutropenia, or ARRs in either treatment arm.

Rituximab exposure (C_{trough} and AUCτ) was slightly higher in patients treated with R-s.c.; however, variability in rituximab exposure was not associated with any safety events in the exposure–safety analysis. Analysis of the pooled data showed no evidence of a relationship between rituximab exposure (C_{tr}LD and C_{mean}LD) and safety events with either R-s.c. or R-i.v. Except for the relationship between C_{mean}LD over the entire induction/treatment period (C1/2–8 (FL) or C1/2–6 (CLL)) with R-i.v. and the probability of any grade ≥ 3 AE, none of the relationships established for the entire induction/treatment period and from C2–8 (FL) or C2–6 (CLL) were statistically significant (i.e., no *P* values < 0.05), and 95% CIs around the 2 logistic regression slopes overlapped with each other, suggesting comparability of the i.v. and s.c. formulations. Logistic regressions for grade ≥ 3 AEs and ARRs are shown in **Figures 3** and **4**, respectively.

DISCUSSION

We describe the successful use of a C_{trough} bridging strategy supported by qCP analyses, and the achievement of clinically effective rituximab exposures with either s.c. or i.v. dosing. In addition to demonstrating noninferior efficacy and comparable safety of the R-s.c. and R-i.v. formulations, the studies included in the analysis collected the largest amount of rituximab clinical pharmacology

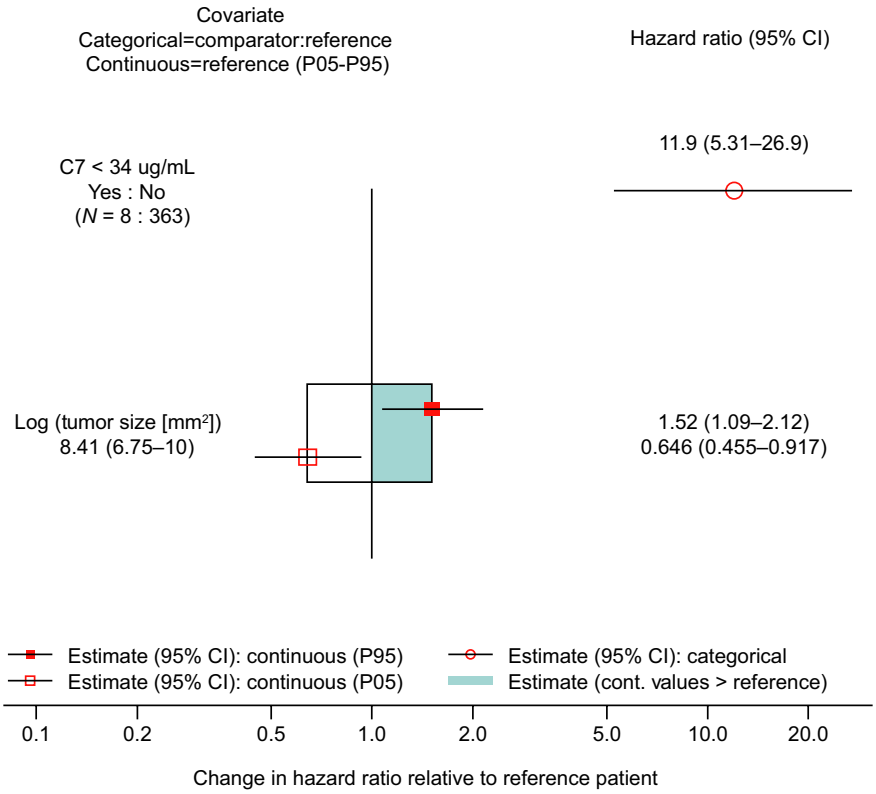

Figure 2 Covariate effects on the hazard ratio for final PFS CPH model in FL. The following covariates were tested in the CPH model: demographic variables (bodyweight, BSA, BMI, age, sex, and race); disease characteristics at baseline (ECOG performance status, time from diagnosis, BSIZ, BM involvement at baseline, symptomatic splenic enlargement, symptomatic hepatic enlargement, Ann Arbor stage at diagnosis, FLIPI); other measures at baseline (WBC, BBCE, and lymphocyte count), route of administration, and concomitant chemotherapy. BBCE, B-cell count at baseline; BM, bone marrow; BMI, body mass index; BSA, body surface area; BSIZ, baseline tumor size; C, cycle; CI, confidence interval; CPH, Cox proportional hazards; ECOG, Eastern Cooperative Oncology Group; FL, follicular lymphoma; FLIPI, Follicular Lymphoma International Prognostic Index; PFS, progression-free survival; WBC, white blood cell count.

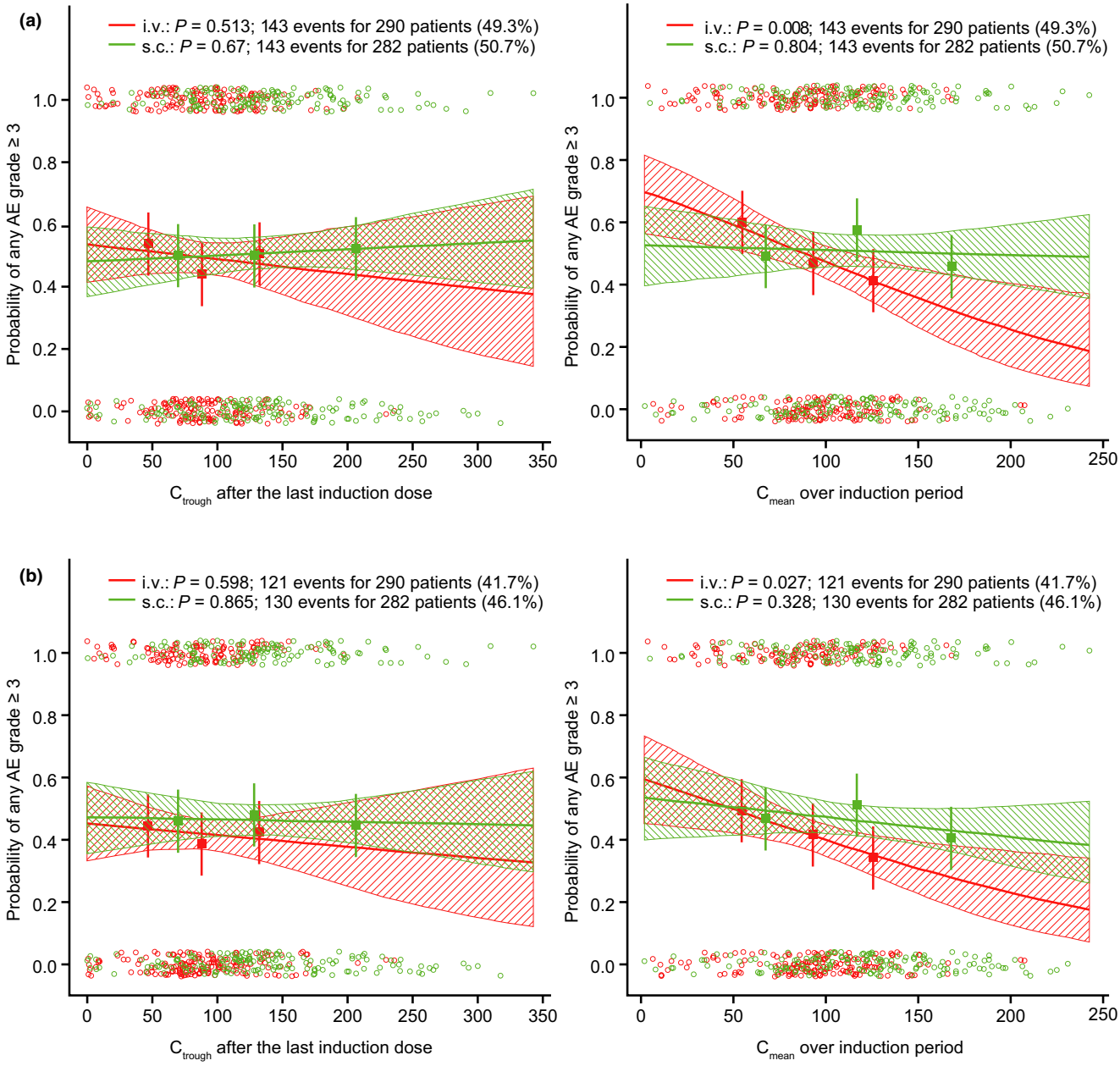

Figure 3 Relationships between probability of any AE grade ≥ 3 and C_{trough} at EOI (FL) or EOT (CLL) (C_{tr}LD) and average concentrations over the induction period (C_{mean}LD). (**a**) Entire induction period. (**b**) From C2 until EOI. Squares and vertical lines show observed fraction of subjects with events in each exposure tertile and 95% CI for these fractions. As all patients received R-i.v. during C1, safety relationships were also examined from C2 to EOI to strictly compare the R-i.v. and R-s.c. formulations. Circles illustrate the observed response (vertically jittered for better visualization). Lines show the logistic regression lines. Shaded regions are the 90% CIs for the regression lines. *P* values are obtained from the glm function of R for the slope of the logistic regression models. Red and green circles represent R-i.v. and R-s.c., respectively. AE, adverse event; C, cycle; CI, confidence interval; C_{mean}, average serum concentration; C_{trough}, minimum serum concentration; EOI, end of induction; EOT, end of treatment; FL, follicular lymphoma; R-i.v., intravenous rituximab; R-s.c., subcutaneous rituximab.

data to date, and enabled a comprehensive assessment of ER relationships for rituximab. Reduced PFS in small numbers of patients with very low exposure is consistent with reports in the literature; reasons for these low exposures are unclear but may be associated with high B-cell count or tumor size. There was no correlation between rituximab exposure and safety events of interest, which supports the use of flat dosing with no need for adjustment for body size. Target receptor saturation is sustained with R-s.c. in both FL and CLL, and the approved R-s.c. dosing regimen achieves the same degree of anti-lymphoma activity as R-i.v. dosing while preserving safety.

Rituximab steady-state C_{trough} used as the primary end point for bridging from i.v. to s.c. dosing

The PopPK analyses of rituximab following i.v. and s.c. administration established that rituximab total clearance included (i) a

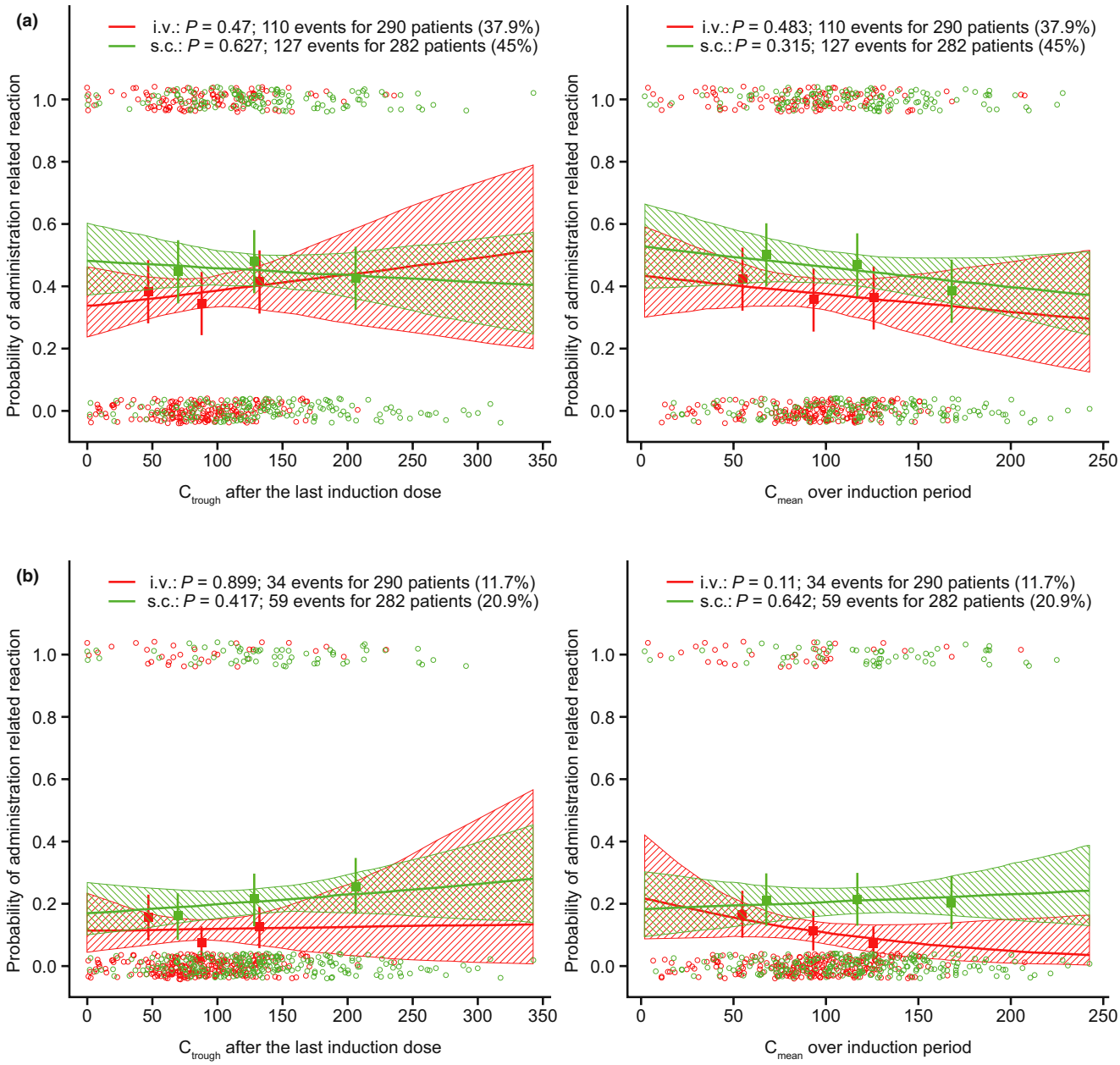

Figure 4 Relationships between probability of ARRs and C_{trough} at EOI (C_{tr}LD) and C_{mean} over induction period (C_{mean}LD). (**a**) For the entire induction period. (**b**) From C2 until EOI. Squares and vertical lines show observed fraction of subjects with events in each exposure tertile and 95% CI for these fractions. Circles illustrate the observed response (vertically jittered for better visualization). Lines show the logistic regression lines. Shaded regions are the 90% CIs for the regression lines. *P* values are obtained from the glm function of R for the slope of the logistic regression models. Red and green circles represent R-i.v. and R-s.c., respectively. ARR, administration-related reaction; C, cycle; CI, confidence interval; C_{mean}, average serum concentration; C_{trough}, minimum serum concentration; EOI, end of induction; R-i.v., intravenous rituximab; R-s.c., subcutaneous rituximab.

first component that decreased exponentially with time following treatment initiation, (ii) a time-independent component (in FL (reported herein) and CLL[26]), and (iii) a third nonlinear elimination component through an additional B-cell compartment (FL only).

It is believed that the CL_T component corresponds to the decrease in capacity of the TMDD related to CD20 target on circulating B cells.[27,36,37] The first-order rate characterizing this clearance decay with time (k_{des}) was similar between FL and CLL, and independent of administration route. Similar to the CL_T component, the nonlinear elimination component in patients with FL (additional component characterized by V_{max}, possibly related to nonrenewable target) was shown to be comparable between R-i.v. and R-s.c. Based on these findings, at the investigated doses, despite significant differences in the rituximab concentration–time course profile between the 2 routes of administration, the times needed to saturate the CD20 receptors in the blood stream (periphery) and the amount of drug eliminated through a potential

additional B-cell compartment were found to be similar between the 2 formulations.

In the current analysis, the PK model has time-varying elimination components (to approximate a TMDD-like behavior), and the use of model parameters (e.g., k_{des} and V_{max}) was optimized to support the comparison of C_{trough} values at EOI.

Consistent with nonlinear elimination, CL_T increased in patients with higher B-cell counts and tumor size. B cells in the periphery represent easily accessible CD20 targets and are depleted first. In contrast, tumor size represents the rituximab target in less accessible tissues. PopPK modeling allows a quantitative understanding of rituximab drug–target interaction and the underlying mechanisms involved in its disposition, thereby providing insight into the link between exposure, target saturation, and expected clinical response. To ensure minimal residual disease secondary to maximal B-cell depletion, a strategy of high CD20 target saturation is desired throughout the dosing interval of rituximab treatment. This approach is consistent with those used for other mAbs associated with antigenic targets and TMDD processes. Several published reports in oncology, rheumatoid arthritis, and chronic inflammatory conditions[38,39] support the utilization of C_{trough} for association with clinical outcomes, and suggest that minimum concentrations exceeding those required for target saturation have been important for mAbs targeting either soluble or membrane bound ligands. Steady-state C_{trough} was therefore a suitable surrogate for exposure, as it reflects the minimum concentration of rituximab over a dosing interval that will maximize peripheral B-cell depletion and duration of CD20 target saturation, thus optimizing response and clinical efficacy.

Comparison of R-s.c. and R-i.v. PKs

Simulations from the PopPK models developed using data from the registration trials, SABRINA and SAWYER, demonstrate that the proposed R-s.c. regimens in FL (375 mg/m^2 i.v. followed by 1,400 mg s.c. Q3W for 8 cycles (induction)) and CLL (500 mg/m^2 i.v. followed by 1,600 mg s.c. Q4W for 6 cycles) have noninferior exposure (C_{trough}) throughout therapy across all BSA groups compared with the approved R-i.v. dosing regimens (375 mg/m^2 Q3W for 8 cycles in FL and 375 mg/m^2 followed by 500 mg/m^2 Q4W for 6 cycles in CLL). Of note, for both FL and CLL, flat s.c. dosing leads to larger differences in exposure between patients with low and high BSA compared with BSA-adjusted i.v. dosing; however, it allows maintenance of rituximab exposure for all BSA groups at least at the levels reached by i.v. dosing, thus achieving noninferior target saturation.

The simulations confirmed that serum rituximab concentrations were sustained over dosing intervals with both routes of administration, and indicate that similar anti-B-cell responses following rituximab treatment will be obtained. Therefore, the same degree of anti-lymphoma activity can be expected irrespective of rituximab administration route in patients with FL and CLL.

Exposure–efficacy analysis

Exposure–efficacy analyses of data from SABRINA and SAWYER stage 2 for PFS supported the overall comparability of efficacy profiles via either administration route, and are consistent with the use of C_{trough} for bridging. As expected, because the investigated R-i.v. and R-s.c. doses led to full target saturation, most patients were found to be at the plateau of effect, and only the small number of patients with low C_{trough} values < 34 μg/mL (FL) or < 32 μg/mL (CLL) were found to have poorer prognosis (notably shorter PFS). However, it is difficult to establish with certainty if low exposure is a cause or a consequence of poor outcome. Most of these patients had high B-cell counts at baseline, indicating high baseline target expression that could explain lower exposure.

In patients with cancer, ER analyses may be confounded by the underlying relationship between exposure and response to treatment, and apparent ER relationships may be response-driven ER relationships, whereby disease-related factors impact PKs. For example, a correlation between cancer cachexia and increased mAb catabolism secondary to generalized protein turnover has been reported for several check-point inhibitors.[40,41] For pembrolizumab, decreased overall survival in patients with higher initial clearance mirrored disease severity markers associated with end-stage cancer anorexia-cachexia syndrome.[40] Thus, increasing the treatment dose (and theoretically concentration) may improve the outcome of patients with low exposure.[42] Several rituximab studies have demonstrated a correlation between lower exposure and inferior outcome;[43,44] however, trials in which increased doses of rituximab were tested have reported mixed results, with some showing no benefit of dose intensification.[43,45–47]

As intrinsic patient and disease characteristics, such as tumor size, are likely to play a role in exposure,[48] lower rituximab exposure (higher CL) may be a consequence of poorer prognosis rather than the cause of poorer clinical outcome as demonstrated previously for rituximab.[49] In the current analysis, only 2.4% and 5.5% of patients with FL and CLL, respectively, seem to be responsible for this apparent exposure–PFS association; indicating that for the majority of patients (97% in FL and > 94% in CLL), variability in exposure does not impact response. To properly assess and resolve the uncertainty surrounding relationships between patient and disease characteristics, exposure, and outcomes, an analysis based on > 1 dose level would be needed, and more potential confounding factors (e.g., CD20 expression) should be considered.[50]

Exposure–safety analysis

Rituximab exposure was not associated with any safety events in the graphical exposure–safety analysis; therefore, the slightly higher exposure seen following R-s.c. dosing vs. established R-i.v. dosing was considered to be within the associated rituximab PK variability[32,33] and was not expected to impact patient safety.

Both separate (CLL (SAWYER) and FL (SABRINA)) and integrated exposure–safety analyses confirmed the lack of association between rituximab exposure and safety events of interest, in accordance with the CLL PopPK analysis of R-i.v. and R-s.c in 255 patients from SAWYER and REACH.[26] Moreover, there was no correlation between rituximab exposure and neutrophil counts, occurrence or grade of neutropenia, or occurrence/frequency of SAEs or grade ≥ 3 AEs following either administration route. The logistic regression analysis indicated the higher the exposure (C_{mean}) the lower the risk of occurrence of grade ≥ 3 AEs. As C_{mean}

was not statistically significantly correlated with the occurrence of other events (particularly ARRs, which are mainly present in C1), the authors did not consider this relationship as clinically relevant. In addition, the slopes of the logistic regressions overlapped for R-i.v. and R-s.c., suggesting no difference in the exposure–safety relationship by route of administration.

CONCLUSIONS

Quantitative pharmacology can provide predictive evidence to optimize a drug's clinical development plan and a safe and effective dosing regimen of a new drug formulation. The modeling approaches applied to rituximab generated evidence for regulatory approval, and enabled faster access to R-s.c.[51] They supported the selection of the R-s.c. dosing regimen and label recommendation, and were of high impact to inform the decision to move forward with an s.c. regimen based on model-informed drug discovery and development principles.[52] Moreover, they enabled simplification of drug administration during therapeutic use expansion of a drug that had been available for almost 2 decades, by integrating solid understanding of its clinical pharmacology into model-informed knowledge.

SUPPORTING INFORMATION

Supplementary information accompanies this paper on the *Clinical Pharmacology & Therapeutics* website (www.cpt-journal.com).

ACKNOWLEDGMENTS

The authors wish to thank Mike Brewster, who was involved in the CLL analysis. Medical writing support, under the guidance of the authors, was provided by Lynda McEvoy, PhD, Ashfield MedComms, an Ashfield Health company, and funded by F. Hoffman-La Roche Ltd.

FUNDING

This analysis was funded by F. Hoffmann-La Roche Ltd.

CONFLICT OF INTEREST

C.J., C.C., P.N.M., C.McI., M.B., L.L., A.Z., A.B., and N.F. are employees of F. Hoffmann-La Roche Ltd. C.J. and C.C. own stock of F. Hoffmann-La Roche Ltd. E.G. and L.G. are contractors of F. Hoffmann-La Roche Ltd.

AUTHOR CONTRIBUTIONS

All authors wrote the manuscript. C.J. and N.F. designed the research. C.J., C.C., E.G., L.G., and M.B. performed the research. E.G., L.G., C.J., C.C., M.B., P.M., C.McI., L.L., A.Z., and A.B. analyzed the data.

DATA SHARING STATEMENT

Qualified researchers may request access to individual patient level data through the clinical study data request platform (https://vivli.org/). Further details on Roche's criteria for eligible studies are available here (https://vivli.org/members/ourmembers/). For further details on Roche's Global Policy on the Sharing of Clinical Information and how to request access to related clinical study documents, see here (https://www.roche.com/research_and_development/who_we_are_how_we_work/clinical_trials/our_commitment_to_data_sharing.htm)

1. Davies, A. *et al*. Subcutaneous rituximab for the treatment of B-cell hematologic malignancies: a review of the scientific rationale and clinical development. *Adv. Ther.* **34**, 2210–2231 (2017).
2. Salles, G. *et al*. Rituximab in B-cell hematologic malignancies: a review of 20 years of clinical experience. *Adv. Ther.* **34**, 2232–2273 (2017).
3. Leandro, M.J. B-cell subpopulations in humans and their differential susceptibility to depletion with anti-CD20 monoclonal antibodies. *Arthritis Res. Ther.* **15**(Suppl 1), S3 (2013).
4. Dreyling, M. *et al*. Newly diagnosed and relapsed follicular lymphoma: ESMO Clinical Practice Guidelines for diagnosis, treatment and follow-up. *Ann. Oncol.* **25**(Suppl 3), iii76–iii82 (2014).
5. Tilly, H. *et al*. Diffuse large B-cell lymphoma (DLBCL): ESMO clinical practice guidelines for diagnosis, treatment and follow-up. *Ann. Oncol.* **26**(Suppl 5), v116–v125 (2015).
6. Eichhorst, B. *et al*. Chronic lymphocytic leukaemia: ESMO clinical practice guidelines for diagnosis, treatment and follow-up. *Ann. Oncol.* **26**(Suppl 5), v78–v84 (2015).
7. NCCN. NCCN Clinical Practice Guidelines in Oncology (NCCN Guidelines®). B-cell lymphomas <https://www.nccn.org/professionals/physician_gls/pdf/b-cell.pdf> (2020). Accessed March 16, 2020.
8. Genentech, Inc. Highlights of prescribing information. Rituxan® (rituximab) injection, for intravenous use <https://www.gene.com/download/pdf/rituxan_prescribing.pdf> (2020). Accessed April 21, 2021.
9. Yelvington, B.J. Subcutaneous rituximab in follicular lymphoma, chronic lymphocytic leukemia, and diffuse large B-cell lymphoma. *J. Adv. Pract. Oncol.* **9**, 530–534 (2018).
10. EMA. MabThera summary of product characteristics <https://www.ema.europa.eu/en/documents/product-information/mabthera-epar-product-information_en.pdf> (2021). Accessed April 21, 2021.
11. Bookbinder, L.H. *et al*. A recombinant human enzyme for enhanced interstitial transport of therapeutics. *J. Control. Release* **114**, 230–241 (2006).
12. Wasserman, R.L. *et al*. Long-term tolerability, safety, and efficacy of recombinant human hyaluronidase-facilitated subcutaneous infusion of human immunoglobulin for primary immunodeficiency. *J. Clin. Immunol.* **36**, 571–582 (2016).
13. Yocum, R.C., Kennard, D. & Heiner, L.S. Assessment and implication of the allergic sensitivity to a single dose of recombinant human hyaluronidase injection: a double-blind, placebo-controlled clinical trial. *J. Infus. Nurs.* **30**, 293–299 (2007).
14. Genentech, Inc. Highlights of prescribing information. Rituxan Hycela® (rituximab and hyaluronidase human) injection, for subcutaneous use <https://www.gene.com/download/pdf/rituxan_hycela_prescribing.pdf> (2021). Accessed April 21, 2021.
15. FDA. Updated information: March 29, 2017: Oncologic Drugs Advisory Committee meeting announcement <https://www.fda.gov/AdvisoryCommittees/Calendar/ucm547160.htm> (2017). Accessed April 21, 2021.
16. Bittner, B. *et al*. Development of a subcutaneous formulation for trastuzumab - nonclinical and clinical bridging approach to the approved intravenous dosing regimen. *Arzneimittelforschung* **62**, 401–409 (2012).
17. Food and Drug Administration. FDA approves new formulation of Herceptin for subcutaneous use <https://www.fda.gov/drugs/drug-approvals-and-databases/fda-approves-new-formulation-herceptin-subcutaneous-use#:~:text=FDA%20approves%20new%20formulation%20of%20Herceptin%20for%20subcutaneous%20use,-Share&text=On%20February%2028%2C%202019%2C%20the,Hylecta%2C%20Genentech%20Inc.> (2019). Accessed April 21, 2021.
18. Venkatakrishnan, K. & Cook, J. Driving access to medicines with a totality of evidence mindset: an opportunity for clinical pharmacology. *Clin. Pharmacol. Ther.* **103**, 373–375 (2018).
19. Davies, A. *et al*. Pharmacokinetics and safety of subcutaneous rituximab in follicular lymphoma (SABRINA): stage 1 analysis of a randomised phase 3 study. *Lancet Oncol.* **15**, 343–352 (2014).

20. Davies, A. *et al*. Efficacy and safety of subcutaneous rituximab versus intravenous rituximab for first-line treatment of follicular lymphoma (SABRINA): a randomised, open-label, phase 3 trial. *Lancet Haematol.* **4**, e272–e282 (2017).
21. Salar, A. *et al*. Comparison of subcutaneous versus intravenous administration of rituximab as maintenance treatment for follicular lymphoma: results from a two-stage, phase IB study. *J. Clin. Oncol.* **32**, 1782–1791 (2014).
22. Assouline, S. *et al*. Pharmacokinetics and safety of subcutaneous rituximab plus fludarabine and cyclophosphamide for patients with chronic lymphocytic leukaemia. *Br. J. Clin. Pharmacol.* **80**, 1001–1009 (2015).
23. Lugtenburg, P. *et al*. Efficacy and safety of subcutaneous and intravenous rituximab plus cyclophosphamide, doxorubicin, vincristine, and prednisone in first-line diffuse large B-cell lymphoma: the randomized MabEase study. *Haematologica* **102**, 1913–1922 (2017).
24. Assouline, S. *et al*. Pharmacokinetics, safety, and efficacy of subcutaneous versus intravenous rituximab plus chemotherapy as treatment for chronic lymphocytic leukaemia (SAWYER): a phase 1b, open-label, randomised controlled non-inferiority trial. *Lancet Haematol.* **3**, e128–e138 (2016).
25. Rummel, M. *et al*. Preference for subcutaneous or intravenous administration of rituximab among patients with untreated CD20+ diffuse large B-cell lymphoma or follicular lymphoma: Results from a prospective, randomized, open-label, crossover study (PrefMab). *Ann. Oncol.* **28**, 836–842 (2017).
26. Gibiansky, E., Gibiansky, L., Chavanne, C., Frey, N. & Jamois, C. Population pharmacokinetic and exposure–response analyses of intravenous rituximab and subcutaneous rituximab in patients with chronic lymphocytic leukemia (CLL). *CPT Pharmacometrics Syst. Pharmacol.* (In Press.).
27. Li, J. *et al*. Population pharmacokinetics of rituximab in patients with chronic lymphocytic leukemia. *J. Clin. Pharmacol.* **52**, 1918–1926 (2012).
28. Ovacik, M. & Lin, K. Tutorial on monoclonal antibody pharmacokinetics and its considerations in early development. *Clin. Transl. Sci.* **11**, 540–552 (2018).
29. Jäger, U. *et al*. Rituximab serum concentrations during immuno-chemotherapy of follicular lymphoma correlate with patient gender, bone marrow infiltration and clinical response. *Haematologica* **97**, 1431–1438 (2012).
30. Igarashi, T. *et al*. Factors affecting toxicity, response and progression-free survival in relapsed patients with indolent B-cell lymphoma and mantle cell lymphoma treated with rituximab: a Japanese phase II study. *Ann. Oncol.* **13**, 928–943 (2002).
31. Tobinai, K. *et al*. Japanese multicenter phase II and pharmacokinetic study of rituximab in relapsed or refractory patients with aggressive B-cell lymphoma. *Ann. Oncol.* **15**, 821–830 (2004).
32. Keating, M. & O'Brien, S. High-dose rituximab therapy in chronic lymphocytic leukemia. *Semin. Oncol.* **27**, 86–90 (2000).
33. O'Brien, S.M. *et al*. Rituximab dose-escalation trial in chronic lymphocytic leukemia. *J. Clin. Oncol.* **19**, 2165–2170 (2001).
34. Robak, T. *et al*. Rituximab plus fludarabine and cyclophosphamide prolongs progression-free survival compared with fludarabine and cyclophosphamide alone in previously treated chronic lymphocytic leukemia. *J. Clin. Oncol.* **28**, 1756–1765 (2010).
35. Beal, S.S., Boeckmann, L. & Sheiner, L.B. *NONMEM user's guides (1989–2009)* (Icon Development Solutions, Elicott City, MA, 2009).
36. Garrett, M., Ruiz-Garcia, A., Parivar, K., Hee, B. & Boni, J. Population pharmacokinetics of inotuzumab ozogamicin in relapsed/refractory acute lymphoblastic leukemia and non-Hodgkin lymphoma. *J. Pharmacokinet. Pharmacodyn.* **46**, 211–222 (2019).
37. Levi, M. *et al*. Characterization of the time-varying clearance of rituximab in non-Hodgkin's lymphoma patients using a population pharmacokinetic analysis. American Conference on Pharmacometrics <https://www.go-acop.org/assets/Legacy_ACOPs/2008ACOP/PostersandAbstracts/levi.pdf> (2008), Accessed October 22, 2020.
38. Kneepkens, E.L. *et al*. Serum tocilizumab trough concentration can be used to monitor systemic IL-6 receptor blockade in patients with rheumatoid arthritis: a prospective observational cohort study. *Scand. J. Rheumatol.* **46**, 87–94 (2017).
39. Cornillie, F. *et al*. Postinduction serum infliximab trough level and decrease of C-reactive protein level are associated with durable sustained response to infliximab: a retrospective analysis of the ACCENT I trial. *Gut* **63**, 1721–1727 (2014).
40. Turner, D.C. *et al*. Pembrolizumab exposure–response assessments challenged by association of cancer cachexia and catabolic clearance. *Clin. Cancer Res.* **24**, 5841–5849 (2018).
41. Bajaj, G. *et al*. Model-based population pharmacokinetic analysis of nivolumab in patients with solid tumors. *CPT Pharmacometrics Syst. Pharmacol.* **6**, 58–66 (2017).
42. Kaagedal, M. *et al*. Herceptin in HER2-positive gastric cancer: evaluation of exposure-response with two dose levels. Population Approach Group in Europe (PAGE) 26 <https://www.page-meeting.org/?abstract=7329> (2017). Accessed April 21, 2021.
43. Pfreundschuh, M. *et al*. Suboptimal dosing of rituximab in male and female patients with DLBCL. *Blood* **123**, 640–646 (2014).
44. Pfreundschuh, M. *et al*. Optimization of rituximab for the treatment of diffuse large B-cell lymphoma (II): extended rituximab exposure time in the SMARTE-R-CHOP-14 trial of the German High-Grade Non-Hodgkin Lymphoma Study Group. *J. Clin. Oncol.* **32**, 4127–4133 (2014).
45. Pfreundschuh, M. *et al*. Optimization of rituximab for the treatment of DLBCL: increasing the dose for elderly male patients. *Br. J. Haematol.* **179**, 410–420 (2017).
46. Lugtenburg, P.J. *et al*. Rituximab–CHOP with early rituximab intensification for diffuse large B-cell lymphoma: a randomized phase III trial of the HOVON and the Nordic Lymphoma Group. *J. Clin. Oncol.* **38**, 3377–3387 (2020).
47. Murawski, N. *et al*. Optimization of rituximab for the treatment of DLBCL (I): dose-dense rituximab in the DENSER-CHOP-14 trial of the DSHNHL. *Ann. Oncol.* **25**, 1800–1806 (2014).
48. Jamois, C. *et al*. Role of obinutuzumab exposure on clinical outcome of follicular lymphoma treated with first-line immunochemotherapy. *Br. J. Clin. Pharm.* **85**, 1495–1506 (2019).
49. Cartron, G. *et al*. Pharmacokinetics of rituximab and its clinical use: thought for the best use? *Crit. Rev. Onc. Hematol.* **62**, 43–52 (2007).
50. Dai, H.I., Vugmeyster, Y. & Mangal, N. Characterizing exposure-response relationship for therapeutic monoclonal antibodies in immuno-oncology and beyond: challenges, perspectives and prospects. *Clin. Pharmacol. Ther.* **108**, 1156–1170 (2020).
51. Nayak, S. *et al*. Getting innovative therapies faster to patients at the right dose: impact of quantitative pharmacology towards first registration and expanding therapeutic use. *Clin. Pharmacol. Ther.* **103**, 378–383 (2018).
52. Marshall, S.F. *et al*. Good practices in model-informed drug discovery and development: Practice, application, and documentation. *CPT Pharmacometrics Syst. Pharmacol.* **5**, 93–122 (2016).